Int. J. Electrochem. Sci., 6 **(2011)** 3844 - 3857

International Journal of
ELECTROCHEMICAL
SCIENCE
www.electrochemsci.org

Electrochemical and Theoretical Studies of Adsorption of Some Indole Derivates at C38 Steel/Sulfuric Acid Interface as Corrosion Inhibitors

M. Lebrini[1], *C. Roos*[1], *H. Vezin*[2], *F. Robert*[1,*]

[1] Laboratoire Matériaux et Molécules en Milieu Amazonien, UAG-UMR ECOFOG, Campus Trou Biran, Cayenne 97337, French Guiana.
[2] Laboratoire de Chimie Organique et Macromoléculaire, UMR-CNRS 8009, USTL BâtC4 F-59655 Villeneuve d'Ascq Cedex, France.
[*]E-mail: florent.robert@guyane.univ-ag.fr

Received: 27 February 2011 / *Accepted:* 25 July 2011 / *Published:* 1 September 2011

The inhibitive action of 9H-pyrido[3,4-b]indole (norharmane) and 1-Methyl-9H-pyrido[3,4-b]indole (harmane) on corrosion of C38 steel in 0.5 M H_2SO_4 solution was investigated through electrochemical techniques. The experimental results obtained revealed that these compounds inhibited the steel corrosion in acid solution for all concentrations studied. Polarization measurements indicate that the examined compounds act as a mixed inhibitor and its inhibition efficiency increases with inhibitor concentration. Data obtained from ac impedance technique show a frequency distribution and therefore a modelling element with frequency dispersion behaviour, a constant phase element (CPE), has been used. The adsorption of used compounds on the steel surface obeys Langmuir's isotherm. The $\Delta G°_{ads}$ values were calculated and discussed for both inhibitors. Significant correlations are obtained between inhibition efficiency and quantum chemical parameters using quantitative structure–activity relationship (QSAR) method.

Keywords: Corrosion inhibitors, C38 steel, acidic media, adsorption, theoretical calculations

1. INTRODUCTION

The study of corrosion of steel and iron is a matter of tremendous theoretical and practical concern has received a considerable amount of interest [1,2]. Several methods are currently used to prevent corrosion of steel. One such method is the use of an organic inhibitor. Effective inhibitors are heterocyclic compounds containing electronegative functional groups, π-electrons and heteroatoms

like sulphur, nitrogen and oxygen as well as aromatic rings in their structure; they often provide excellent corrosion inhibition of steel in acid media [3–10]. The inhibitor films can be classified as a chemisorbed film, donating a lone pair of electrons attached to a central adsorption atom in a functional group, as an electrostatic adsorption film and as a precipitation and/or a complex film, reacting with dissolved metal ion and organic inhibitor molecule [11]. Survey of literature reveals that indole compounds are also effective corrosion inhibitors for steel and copper in acidic solutions [12–16]. This work presents the experimental data obtained by potentiodynamic polarization and electrochemical impedance spectroscopy on the behavior of some indole derivates namely, 9H-pyrido[3,4-b]indole (norharmane) and 1-Methyl-9H-pyrido[3,4-b]indole (harmane) on the inhibition of corrosion of C38 steel in 0.5 M H_2SO_4 solution at 25 °C. Adsorption mode and corrosion inhibition mechanism on the steel surface are discussed. We have performed molecular modelling using the linear resistance (LR) model in order to understand if any structural differences between the molecules can be reliable to the experimental inhibition efficiencies. Highly significant correlation coefficients ($R^2 > 0.97$) have been obtained using the proposed model.

2. EXPERIMENTAL

2.1. Electrode and solution

The sample selected for the study was C38 steel. Steel strips containing 0.36 wt% C, 0.66 wt% Mn, 0.27 wt% Si, 0.02 wt% S, 0.015 wt% P, 0.21 wt% Cr, 0.02 wt% Mo, 0.22 wt% Cu, 0.06 wt% Al and the remainder iron.The specimens were embedded in epoxy resin leaving a working area of 0.78 cm2. The working surface was subsequently polished with 180, 600 and 1200 grit abrading papers, cleaned by distilled water and ethanol. The 0.5 M H_2SO_4 solutions were prepared by dilution of an analytical reagent grade 87% H2SO4 with doubly distilled water. All the tests were performed at ambient temperature (25 °C). The tested inhibitors are 9H-pyrido[3,4-b]indole (norharmane) and 1-Methyl-9H-pyrido[3,4-b]indole (harmane); their molecular structures are shown in Figure 1. The investigated compounds were commercial products: norharmane (Aldrich, P99%), harmane (Sigma, P98%), the concentration range of inhibitor employed was 0.2 mM to 1.2 mM. The choice of these compounds was based on molecular structure considerations; it's an organic compound with an adsorption centre.

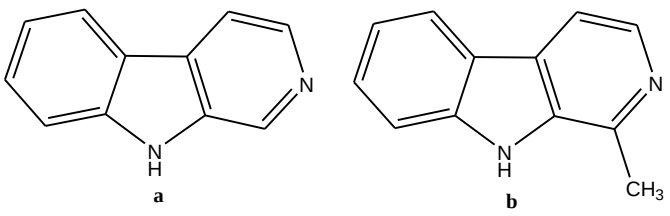

Figure 1. Chemical formulas of the tested inhibitors; a) norharmane and b) harmane.

2.2. Electrochemical measurements

Electrochemical measurements were performed in a three-electrode cell on C38 steel specimen, a platinum wire as the counter and a saturated calomel electrode (SCE) as the reference. Before each LP and EIS experiments, the electrode was allowed to corrode freely and its open circuit potential (OCP) was recorded as a function of time for 3 h, the time necessary to reach a quasi-stationary value for the open-circuit potential. The polarisation curves were recorded with a scan rate 20 mV/min. All potentials are reported vs. SCE. Ac impedance measurements were performed using a Bio-Logic system frequency response analyzer in a frequency range of 10^5 Hz to 10^{-2} Hz with five points per decade using 5 mV peak-to-peak sinusoidal voltage. Electrochemical measurements were performed using a VSP electrochemical measurement system (Bio-Logic). The above procedures were repeated two times with success for each concentration of the two tested inhibitors. The Tafel and EIS data were analysed using graphing and analyzing impedance software, version EC-Lab V9.97.

2.3. Theoretical calculation.

Quantum chemistry was performed using Gaussian 03 program using Density Functional Theory formalism. Geometry of protonated compounds were fully optimized without any constraints using hybrid B3LYP functional and 6-31G(2d,2p) basis set in solvent (water) using polarize continuum model PCM model. The following quantum chemical indices were considered: the energy of the highest occupied molecular orbital (E_{HOMO}), the energy of the lowest unoccupied molecular orbital (E_{LUMO}), $\Delta = E_{HOMO} - E_{LUMO}$ and the dipole moment (μ).

3. RESULTS AND DISCUSSION

3.1. Polarisation curves

Figs. 2 and 3 show a typical record of Tafel polarization measurements for C38 steel in 0.5 M H_2SO_4 in the absence and presence of the indole derivates at 25 °C. From these figures, it can be seen that addition of the harmane to acid media affected both the cathodic and anodic parts of the curves. In the presence of norharmane; the cathodic reaction is remarkably affected, whereas the anodic one is slightly shifted toward lower currents at law concentration. It is clear that corrosion current density decreased with increasing the concentration of the inhibitors. Table 1 lists the polarization parameters for corrosion of C38 steel in the presence of different concentrations of the investigated inhibitors. The polarization resistances (R_p) were calculated from the linear *I-E* plots in the potential range ±25 mV from the corrosion potential. The R_p fit was obtained with a good correlation coefficient ($R^2 \geq 0.999$). The corresponding R_P values are also given in Table 1. It is found (Table 1) that, as the indole derivates concentration increases, the polarization resistances values increase, while the corrosion current density values tend to decrease. Corrosion potential shifted to negative direction; although there was not a specific relation between E_{corr} and inhibitors concentration. Since the largest

displacement exhibited by norharmane and harmane is 10 and 23 mV, respectively. This negative shift indicates that norharmane and harmane inhibit acid corrosion of steel with predominantly control the cathodic reaction. Therefore, these compounds behave as mixed-type inhibitors. *IE*(%) increased with inhibitor concentration reaching a maximum value at 1.2 mM for both inhibitors. The inhibition efficiencies calculated from R_p results show the same trend as those obtained from I_{corr}. The harmane molecule gives more inhibition efficiency than norharmane mainly at low concentrations, this enhanced efficiency may be due to the replacement of hydrogen atom in pyridine of norharmane molecule by an alkyl group ($-CH_3$); such group having inductive effect (+I), would assist increasing electron density and arises an enhancement in the inhibition efficiency.

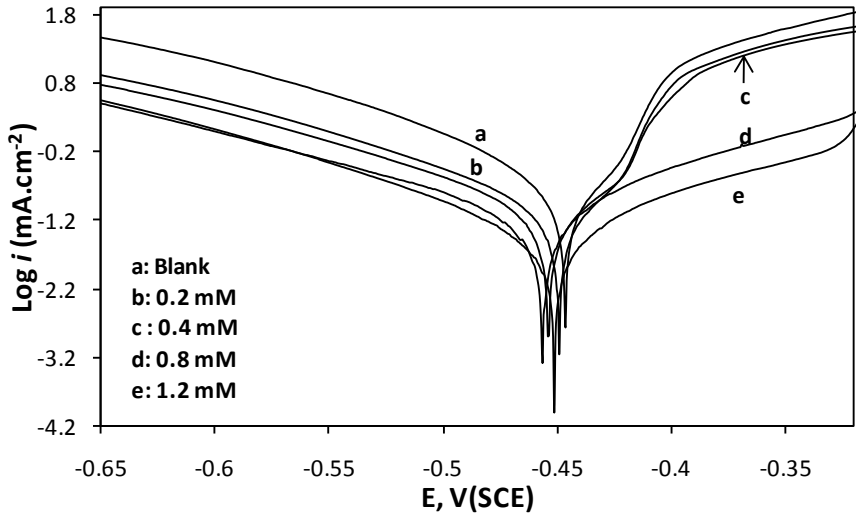

Figure 2. Polarisation curves for C38 steel in 0.5 M H_2SO_4 containing different concentrations of norharmane.

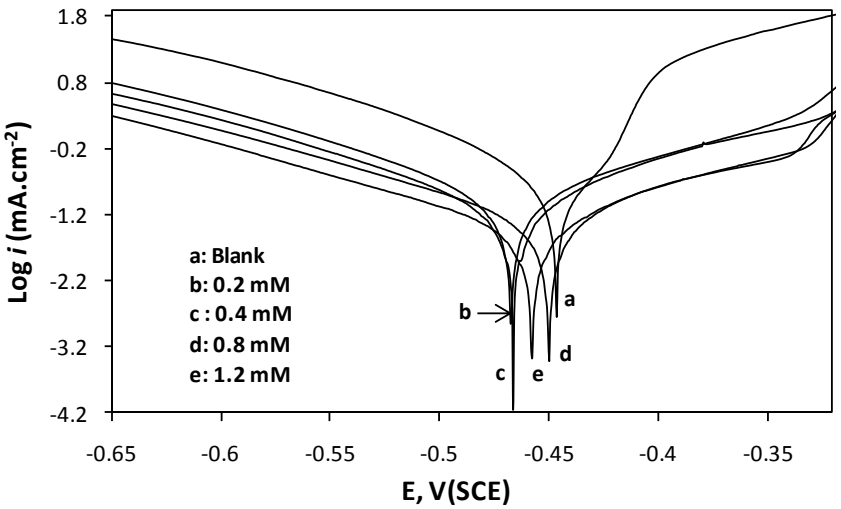

Figure 3. Polarisation curves for C38 steel in 0.5 M H_2SO_4 containing different concentrations of harmane.

Table 1. Polarization parameters and the corresponding inhibition efficiency for the corrosion of C38 steel in 0.5 M H_2SO_4 containing different concentrations of harmane and norharmane at 25 °C.

Concentration mM	E_{corr} vs SCE	I_{corr}	R_p	IE $_{Icorr}$	IE $_{Rp}$
	(mV)	(μA cm^{-2})	(Ω cm^2)	(%)	(%)
0.5 M H_2SO_4	-446	438	42	—	—
norharmane					
0.2	-449	127	149	71	72
0.4	-453	96	171	78	75
0.8	-456	82	245	81	83
1.2	-450	56	300	87	86
harmane					
0.2	-469	93	175	75	76
0.4	-465	76	228	83	81
0.8	-449	56	340	87	87
1.2	-458	48	400	89	89

3.2. Electrochemical impedance spectroscopy (EIS)

Figs. 4 and 5 show typical set of complex plane plots of C38 steel in 0.5 M H_2SO_4 solution in the absence and in the presence of different concentrations of the indole derivates at 25 °C. It is clear that all of the impedance spectra obtained consist of one depressed capacitive loop corresponding to one time constant in Bode plots (Fig. 6, representative example). It is obvious that addition of inhibitors results in an increase in the diameter of the semicircular capacitive loop (Figs. 4 and 5), in the impedance of the double layer (Fig. 6a) and in the maximum phase angle (Fig. 6b). Inspections of the data reveal that the Nyquist plot obtained for both inhibitors seems to present a depressed loop, such behaviors are mostly referred as the frequency dispersion and they are attributed to irregularities and heterogeneities of the solid surfaces [17-21]. In particular, the high frequency part of the impedance and phase angle reflects the behavior of heterogeneous surface layer whereas the low frequency part shows the kinetic response for the charge transfer reaction [22]. In such cases, the parallel combination of double layer capacitance and charge transfer resistance which are in series with solution resistance ($R_s(C_{dl}R_{ct})$), particularly in the presence of an efficient inhibitor, is found to be an inadequate approach for modeling the interface. The use of the constant phase element (CPE) can be an effective way to represent the frequency dependence of non-ideal capacitive behavior. The impedance of the CPE is given by [23,24]:

$$Z_{CPE} = A^{-1}(i\omega)^{-n} \qquad (1)$$

In order to obtain accurate results the analysis of complex plane plots was done by fitting the experimental results to the equivalent circuit given in Fig. 7, which has been used previously to model the mild steel/acid interface [25–28]. The circuit consists of solution resistance (R_s) in series with the parallel combination of charge transfer resistance (R_{ct}) and a constant phase element, CPE used in place of double layer capacitance (C_{dl}) to represent the non-ideal capacitive behavior of the double layer more clearly. The results obtained from these complex plane plots are given in Table 2. A good fit with the proposed model was obtained with our experimental data (Fig. 6; representative example). It's observed that an acceptable accuracy of the fitting was obtained, as evidence by Chi-square in the order of 10^{-3} for all the experimental data. Estimates of the margins of error calculated for the parameters are also presented in Table 2. The calculated values of C_{dl} using the equation (2) [24,29-30] and the relaxation time using the equation (3) [46,48] are also shown in the same Table.

$$C_{dl} = (A.R_{ct}^{1-n})^{1/n} \quad (2)$$

$$\tau = C_{dl} R_{ct} \quad (3)$$

From Table 2, it is apparent that the charge transfer resistance (R_{ct}) value of C38 steel in uninhibited solution increases significantly after the addition of indole derivates. Also the addition of indole derivates to the corrosive solution decreases the double layer capacitance. The double layer between the charged metal surface and the solution is considered as an electrical capacitor. The decrease in this capacity could be attributed to the adsorption of the inhibitors forming protective adsorption layers on the metal surface [31]. The calculated values of the time constant (τ) obtained in the presence of both inhibitors were found to be higher than that uninhibited solution.

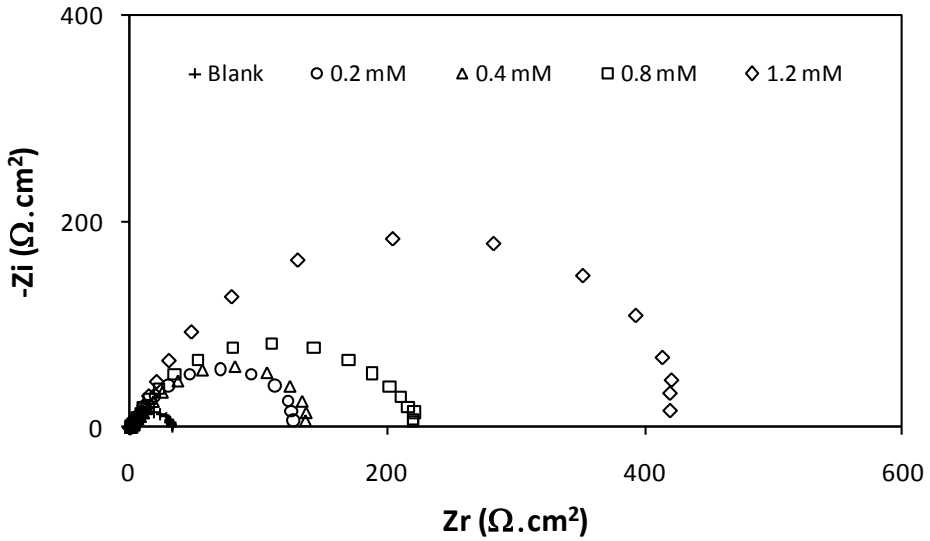

Figure 4. Nyquist plots for C38 steel in 0.5 M H_2SO_4 in the absence and presence of different concentrations of norharmane.

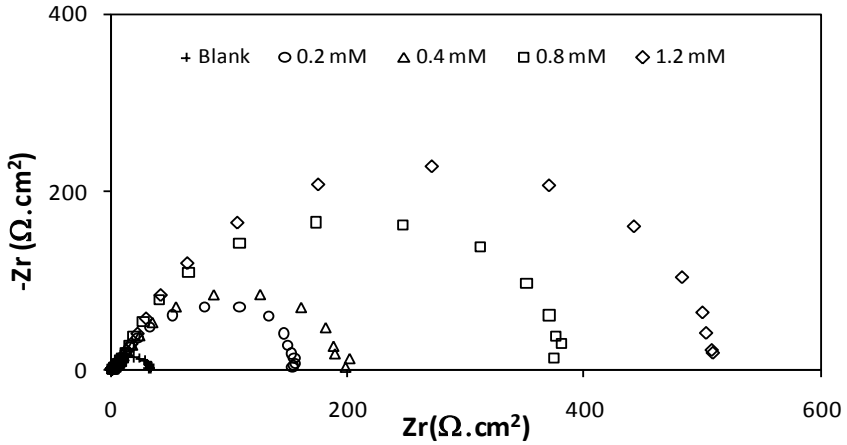

Figure 5. Nyquist plots for C38 steel in 0.5 M H_2SO_4 in the absence and presence of different concentrations of harmane.

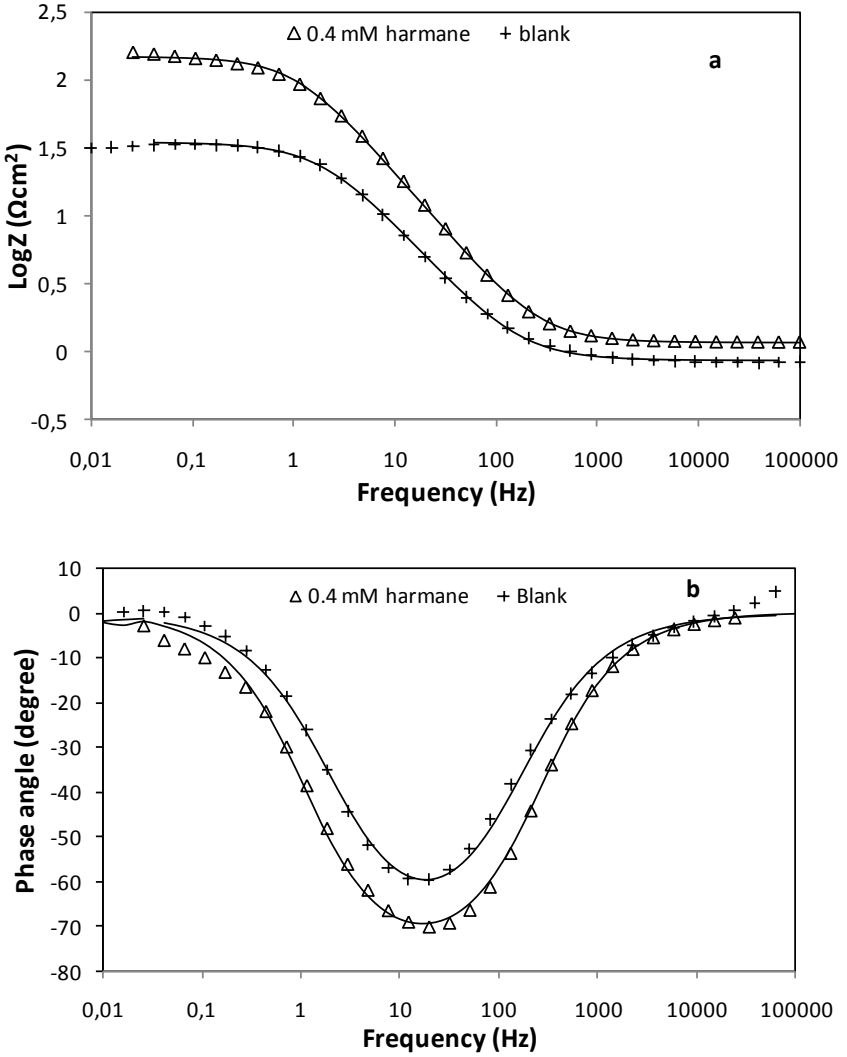

Figure 6. Bode plots, (a) LogZ vs. freq and (b) phase angle vs. freq for C38 steel in 0.5 M H_2SO_4 solution in the absence and in the presence of 0.4 mM harmane; (Δ; +), Experimental results and (—), fit results.

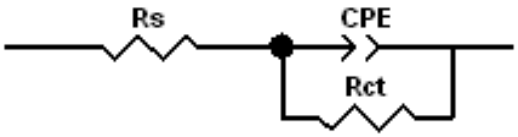

Figure 7. Equivalent circuit model represents the metal/solution interface; CPE: constant phase element; R_{ct}: charge transfer resistance and R_s: solution resistance.

Table 2. Values of the elements of equivalent circuit required for fitting the EIS for C38 steel in 0.5 M H_2SO_4 in the absence and presence of different concentrations of indole derivates and the corresponding inhibition efficiency.

Concentration (mM)	R_{ct}	10^4 A	n	C_{dl}	τ_d	IE
	(Ω cm^2)	(Ω^{-1} s^n cm^{-2})		(μF cm^{-2})	(s)	(%)
0.5 M H_2SO_4	33 ± 2.35	22.59 ± 1.78	0.798 ± 0.14	1170	0.0386	—
norharmane						
0.2	131 ± 1.01	10.9 ± 0.45	0.821 ± 0.10	713	0.1050	75
0.4	156 ± 1.32	8.12 ± 0.41	0.846 ± 0.09	557	0.1151	79
0.8	223 ± 0.99	7.02 ± 0.18	0.857 ± 0.38	515	0.1963	85
1.2	434 ± 1.09	5.85 ± 0.32	0.869 ± 0.51	476	0.2135	90
harmane						
0.2	156 ± 0.86	8.96 ± 1.21	0.873 ± 0.08	673	0.0934	79
0.4	209 ± 2.54	7.99 ± 0.75	0.828 ± 0.03	551	0.0870	84
0.8	390 ± 1.65	6.05 ± 0.21	0.887 ± 0.21	503	0.1149	91
1.2	508 ± 5.41	5.05 ± 0.61	0.881 ± 0.53	420	0.2065	93

3.3. Adsorption Isotherm

In order to understand the mechanism of corrosion inhibition, the adsorption behavior of the organic adsorbate on the steel surface must be known. The degree of surface coverage (θ) for different concentration of inhibitors has been evaluated from AC impedance study. The data were tested graphically by fitting to various isotherms including Langmuir and Frumkin (Figs. 8 and 9). According to these isotherms, θ is related to the inhibitor concentration C_{inh} via:

$$\frac{C_{\text{inh}}}{\theta} = \frac{1}{K} + C_{\text{inh}} \qquad \text{(Langmuir isotherm)} \qquad (4)$$

$$\left(\frac{\theta}{1-\theta}\right)\exp(-2a\theta) = KC_{\text{inh}} \qquad \text{(Frumkin isotherm)} \qquad (5)$$

where K is the binding constant of the adsorption reaction and "a" is the lateral interaction term describing the molecular interactions in the adsorption layer and the heterogeneity of the surface.

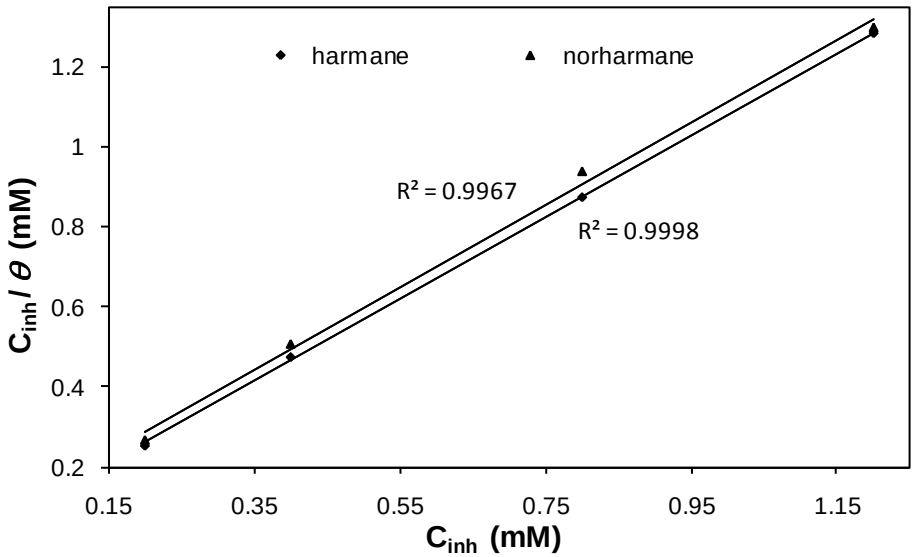

Figure 8. Langmuir adsorption plots for C38 steel in 0.5 M H_2SO_4 containing different concentrations of norharmane and harmane.

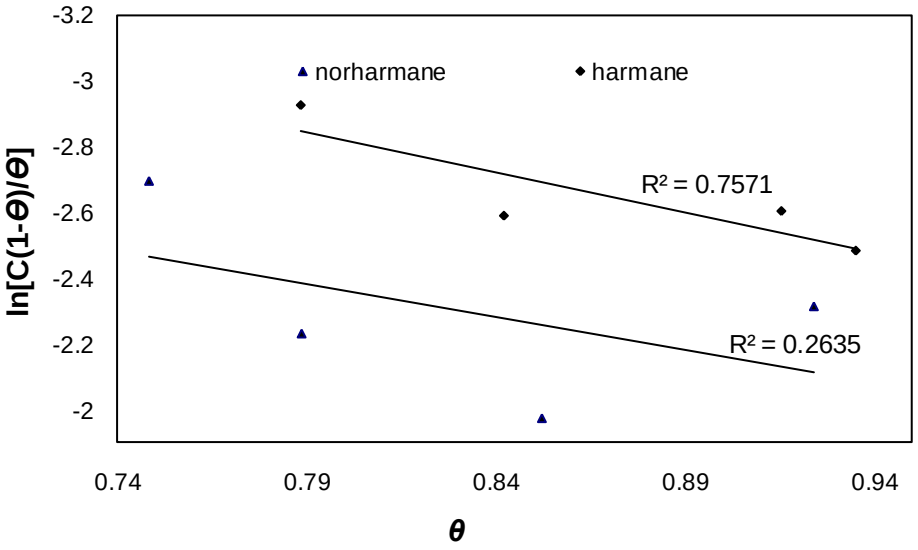

Figure 9. Frumkin adsorption plots for C38 steel in 0.5 M H_2SO_4 containing different concentrations of norharmane and harmane.

By far the best fit was obtained with the Langmuir isotherm. The plots of C_{inh}/θ vs. C_{inh} yield a straight line, where C_{inh} is the inhibitor concentration (Fig. 8). These results indicate that the adsorption of the norharmane and harmane from 0.5 M H_2SO_4 solution on the C38 steel surface corresponded to the Langmuir isotherm model. From the intercepts of the straight lines C_{inh}/θ – axis, K values can be

calculated. The constant of adsorption (K) is related to the standard free energy of adsorption (ΔG^0_{ads}) with the equation (6) [33].

$$K = \frac{1}{55.5}\exp\left(\frac{-\Delta G^0_{ads}}{RT}\right) \quad (6)$$

The values of the free energy of the adsorption as calculated from the Langmuir-type adsorption isotherm for norharmane and harmane in 0.5 M H_2SO_4 were −15 kJ mol^{-1} and −14 kJ mol^{-1}, respectively. The obtained $\Delta G°_{ads}$ indicate that the adsorption mechanism of norharmane and harmane on C38 steel surface involves a physisorption. It means that, the inhibitors are able to electrostatically adsorb on the charged metal. Since the organic compounds used as inhibitors in this work are polar (4.05 and 4.13 Debye for harmane and norharmane, respectively), the electrostatic interaction between the electric field, due to the metal charge, and electric moment of the molecule probably contribute to the adsorption. In our case, the indole derivatives are organic bases, which can be protonated in an acid medium.

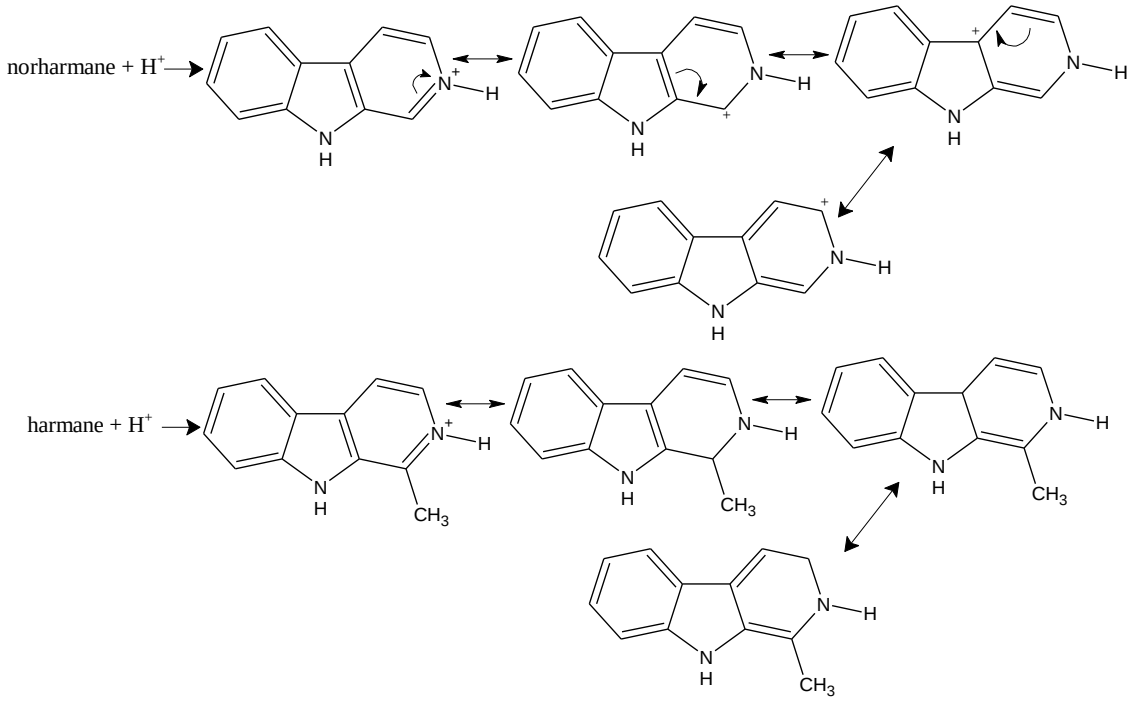

Figure 10. Withdrawing effect of pyridinium substituent in indole molecules.

The harmane and norharmane molecules exist in the form of protonated species (Fig. 10). It can be seen that in indole molecules, no direct withdrawing effect can be observed by the pyridinium substituent on the pyrrole ring. Even the acidity of the medium, pyridine of indole does not remain in solution as free bases. Therefore, it may be assumed that, the first contact between the metal surface and indole derivates is between charged metal and pyridinium ions. On the other hand; it appears that

replacement of hydrogen atom in pyridine of norharmane molecule by alkyl group ($–CH_3$) having inductive effect (+I), would assist increasing electron density. Thus, such group arises an enhancement in the inhibition efficiency. For this reason, the highest inhibition efficiency values were found for harmane.

Indeed, upon increasing the concentration of inhibitors, the time of adsorption process becomes much higher which means slow adsorption process [32]. The data of *n* were generally higher in the inhibited solutions than that uninhibited ones and this is interpreted as an evidence for surface homogeneity increase, due to the adsorption of inhibitor onto the steel surface. The value of the parameter *A* of the Z_{CPE} varies in a regular manner with concentration. The inhibition efficiency values, calculated from ac impedance study, show the same trend as those obtained from polarization techniques. It is found that *IE*(%) increases with the inhibitor concentration. The excellent behaviour of indole derivates previously evidenced in the polarisation curves measurement was again confirmed by AC impedance study. The highest efficiency values were calculated for harmane, due to the similar raison given in the polarisation curves paragraph.

3.4. Electronic Properties and Quantitative Structure Activity Relationship

The general equation describing our studied QSAR linear model can be expressed as follows [34]:

$$1/R_{t_i} = \sum_j (A\,\mu_j + B\,E_{HOMO_j} + C\,E_{LUMO_j})\,C_{inh_i} \quad \text{(LR)} \qquad (7)$$

where R_t is the charge transfer resistance, A, B, and C are the regression coefficients of the calculated quantum chemical parameters for the molecule j and $C_{inh,i}$ denotes the concentration of the inhibitor in experiment i.

The calculated quantum chemical indices (E_{HOMO}, E_{LUMO} and μ) for indole derivates are reported in Table 3. As these two indole structures contain ionizable nitrogen at acidic pH; the calculation have been taking account of the solvent effect and compared with these obtained in vacuum. The calculated pKa values, with the Sparc online calculator, were found 4.81 and 5.57 for harmane and norharmane, respectively. This result proves that the cationic forms of both molecules in 0.5 M H_2SO_4 media are realistic [35]. Experimental and calculated values of the inverse of R_{ct} are displayed in Fig. 11. The best regression equation for this family (non protonated forms; Eq. 8 and protonated forms; Eq. 9), obtained by using the LR model was:

$$R_{ct} = 150 + (-359539\,E_{HOMO} + 1585825\,E_{LUMO})\,C_{inh} \qquad (8)$$
$$R^2 = 0.97, \qquad F = 54$$

$$R_{ct} = 150 + (-402535\,E_{HOMO} + 960146\,E_{LUMO})\,C_{inh} \qquad (9)$$
$$R^2 = 0.97, \qquad F = 54$$

where R^2 denotes the multiple correlation coefficient. The significance of the regression equation was obtained by calculating the Fischer's number (F) [36]. As shown in Fig. 11, the correlation between experimental and estimated values of $1/R_t$ of the two indole derivatives was better using the LR model (R^2 = 0.97) for both forms. In this correlation we can observe that the inhibition corrosion efficiency is mainly supported only by the LUMO and HOMO coefficients. The dipole moment not participates in the structure-activity relationship. In vacuum calculation, the results show that the effect of HOMO and LUMO energies are quite in the same order of magnitude for the correlation with a negative coefficient for HOMO energy and a positive one for the LUMO energy. The LUMO coefficient is higher than HOMO one, indicating an acceptance effect tendency. For the correlation performed by introducing the solvent effect, the same behavior is observed except for coefficients which are lower for both HOMO and LUMO energies and therefore indicating an increase of acceptance character.

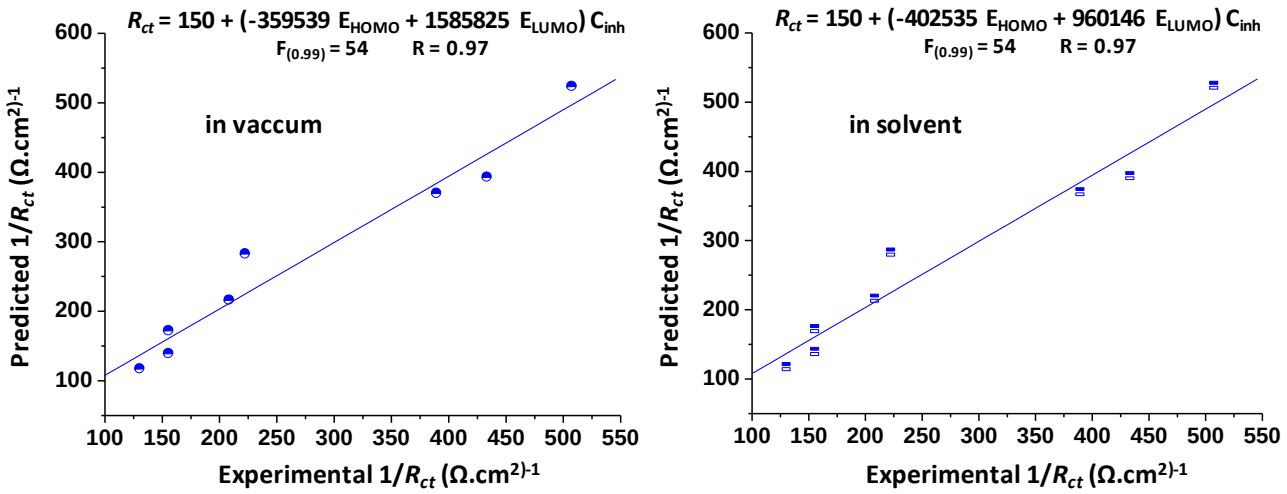

Figure 11. Experimental and predicted $1/R_{ct}$ values of protonated (in solvent) and non protonated (in vaccum) molecules calculated by LR using E_{HOMO} and E_{LUMO} as quantum descriptors.

Table 3. Calculated quantum chemical indices for harmane, norhamane and for the protonated species.

Inhibitor	E_{HOMO} (eV)	E_{LUMO} (eV)	ΔE (eV)	μ (debye)
non protonated harmane	-5.58	-1.02	-4.56	4.05
protonated harmane $^+$	-6.30	-2.24	-4.06	8.73
non protonated norharmane	-5.64	-1.10	-4.54	4.13
protonated norharmane $^+$	-6.36	-2.38	-3.98	9.38

There is an obvious contradiction between the results of experimental witness and the finding of theoretical approach; the first indicates the inhibitor molecules being physisorbed (see mechanism

of inhibition, Adsorption Isotherm paragraph) whereas the latter suggest chemisorptions. If we accept that the physical forces are exerted between the inhibitor molecules and the metal surface then we should observe a correlation between inhibition efficiency and electrical dipole moment (a criterion for physical/electrostatic interactions). By contrast, the theory declines this expectation and exhibits a significant correlation with the quantities HOMO and LUMO, which both are important for chemical bond formation through the electron sharing.

This allows us to suppose that a chemisorption is possible. It may be assumed that, the first contact between the metal surface and indoles is between metal and pyridinium ions. As corrosion begins, the cation may become attached to the anodic sites, otherwise, the alkalinity produced at the cathodic sites may reform the free base, and thus, the adsorption of the indoles on the metal surface can occur directly via donor-acceptor interactions between the π-electrons of the heterocyclic compound and the vacant "d" orbitals of iron surface atoms.

4. CONCLUSION

Polarization measurement and electrochemical impedance spectroscopy results indicated that inhibition efficiency increased with the inhibitor concentration. The inhibition efficiency obtained using different techniques showed a good agreement with each other. The inhibiting action of these compounds was attributed to blocking of the electrode surface by adsorption through its active centers. Based on the polarization results, the investigated indoles can be classified as mixed inhibitors. Data obtained from ac impedance technique show a frequency distribution and therefore a modelling element with frequency dispersion behaviour, a constant phase element (CPE) has been used. Adsorption of the inhibitors fits a Langmuir isotherm model. Highly significant multiple correlation coefficients have been obtained between experimental and predicted $1/R_t$ using the proposed model. Theoretical calculations show that the effect of the two molecules studied on inhibition of C38 steel in acidic solution could be mainly attributed to quantum chemical parameters.

ACKNOWLEDGEMENT
This work was supported by European Union through DEGRAD framework (FEDER funds, PRESAGE 30070).

References

1. V.S. Sastri, *Corrosion Inhibitors: Principles and Application*, John Wiley and Sons, New York, (1998) p 25
2. H.H. Uhlig, R.W. Revie, *Corrosion and Corrosion Control*, John Wiley, New York, (1985) p 78
3. N.O. Eddy, E. E. Ebenso, *Int. J. Electrochem. Sci.* 5 (2010) 731.
4. B.M. Praveen, T.V. Venkatesha, *Int. J. Electrochem. Sci.* 4 (2009) 267.
5. M.G. Hosseini, M.R. Arshadi, *Int. J. Electrochem. Sci.* 4 (2009) 1339.
6. O.K. Abiola, J.O.E. Otaigbe, *Int. J. Electrochem. Sci.* 3 (2008) 191.
7. M. Lebrini, F. Robert, C. Roos, *Int. J. Electrochem. Sci.* 5 (2010) 1698.

8. X. Joseph Raj, N. Rajendran, *Int. J. Electrochem. Sci.* 6 (2011) 348.
9. M. Lebrini, F. Robert, C. Roos, *Int. J. Electrochem. Sci.* 6 (2011) 847.
10. A.Zarrouk, T. Chelfi, A. Dafali, B. Hammouti, S.S. Al-Deyab, I. Warad, N. Benchat, M. *Int. J. Electrochem. Sci.* 5 (2010) 696.
11. Hamner NE in: C.C. Nathan (Ed.), *Corrosion Inhibitors*, Nace Houston, Texas, USA, (1973) p. 1.
12. M. Lebrini, F. Robert, H. Vezin, C. Roos, *Corros. Sci.* 52 (2010) 3367.
13. A.A. Ismail, S.H. Sanad, A.A. El- Meligi, *J Mater Sci Technol* 16 (2000) 397.
14. A.A. El- Meligi, S. Turgoose, A.A. Ismail, S.H. Sanad, *Br. Corros. J.* 35 (2000) 75.
15. G. Moretti, F. Guidi, *Corros Sci* 44 (2002)1995.
16. T. Tuken, M. Düdükcü, B. Yazici, M. Erbil, *Prog. Org. Coat.* 50 (2004) 273.
17. Z.B. Stoynov, B.M. Grafov, B.S. Stoynova, V.V. Elkin, *Electrochemical Impedance*, Nauka, Moscow (1991).
18. F.B. Growcock, R.J. Jasinski, *J. Electrochem. Soc*.136 (1989) 2310.
19. G. Reinhard, U. Rammelt in: Proc 6th *European Symposium on Corrosion Inhibitors* Univ. Ferrara, (1985) p. 831.
20. P. Li, J.Y. Lin, K.L. Tan, J.Y. Lee, *Electrochim. Acta* 42 (1997) 605.
21. D.A. Lopez, S.N. Simison, S.R. de Sanchez, *Electrochim. Acta* 48 (2003) 845.
22. M.S. Morad, *Corros. Sci.* 42 (2000) 1307.
23. Z. Stoynov, *Electrochim. Acta* 35 (1990) 1493.
24. S. Martinez, M.M. Hukovic, *J. Appl. Electrochem.* 33 (2003) 1137.
25. A.Popova, S. Raicheva, E. Sokolova, M. Christov, *Langmuir* 12 (1996) 2083.
26. A.Popova, E. Sokolova, S. Raicheva, M. Christov, *Corros. Sci.* 45 (2003) 33.
27. A.Popova, M. Christov, *Corros. Sci.* 48 (2006) 3208.
28. A.Popova, *Corros. Sci.* 49 (2007) 2144.
29. X. Wu, H. Ma, S. Chen, Z. Xu, A. Sui, *J. Electrochem. Soc.* 146 (1999) 1847.
30. H. Ma, X. Cheng, G. Li, S. Chen, Z. Quan, S. Zhao, L. Niu, *Corros. Sci.* 42 (2000) 1669.
31. Z.O.R. Sibel, P. Dogan, B. Yazici, *Corros. Rev.* 23 (2005) 217.
32. M.S. Morad, *Corros. Sci.* 50 (2008) 436.
33. J. Flis, T. Zakroczymski, *J. Electrochem. Soc.* 143 (1996) 2458.
34. F. Bentiss, M. Traisnel, M. Lagrenée, H. Vezin, *Corros. Sci.* 45 (2003) 371.
35. S. Hilal, S.W. Karickhoff, L.A. Carreira, Quant. Struc. Act. Rel. 14 (1995) 348.
36. G.W. Snedecor, W.G. Cochran, *Statistical Methods*, Iowa State University Press, Ames, IA, (1972) p. 117.